

CAAP Quarterly Report

Date of Report: *June 30, 2020*

Contract Number: 693JK31850012CAAP

Prepared for: *USDOT Pipeline and Hazardous Materials Safety Administration (PHMSA)*

Project Title: *Magnet-assisted Fiber Optic Sensing for Internal and External Corrosion-induced Mass losses of Metal Pipelines under Operation Conditions*

Prepared by: *Missouri University of Science and Technology (Missouri S&T)*

Contact Information: *Genda Chen, Ph.D., P.E., Email: gchen@mst.edu, Phone: (573) 341-4462*

For quarterly period ending: *June 30, 2020*

Business and Activity Section

(a) General Commitments – Dr. Genda Chen directed the entire project and coordinated various project activities.

Dr. Chuanrui Guo, postdoctoral research fellow, and Mr. Ying Zhuo, Ph.D. candidate in civil engineering at Missouri S&T, were on board for this project. They are responsible for the fabrication and characterization test of sensors under Dr. Chen's supervision.

(b) Status Update of Past Quarter Activities – Detailed updates are provided below by task.

Task 1 Optimization of a magnet-assisted hybrid FBG/EFPI sensor enclosed in a plexiglass container for simultaneous measurement of temperature and pipe wall thickness

Task 1 was completed in the fourth quarter of 2019.

Task 2 Development and validation of a graphene-based LPFG sensor with Fe-C coating for improved sensitivity in mass loss measurement in varying temperature environment

To characterize the attenuation of evanescent field in radial direction of optic fibers, three long period fiber gratings (LPFG) sensors coated with a varying number of graphene (Gr) layers were prepared and tested. Monolayer Gr was first synthesized on the top side of a copper (Cu) foil through a low pressure chemical vapor deposition (LPCVD) system. The Gr/Cu sample was then coated by a thin uniform layer of Poly(methyl methacrylate) (PMMA, $M_w=996,000$, Sigma Aldrich) as a "tape" to make graphene fragments stick together. Next, the sample was floated on the copper etchant solution for 4 hours to dissolve the copper foil and obtain a PMMA/Gr transparent film. The PMMA/Gr transparent film, while floating in the solution, was supported underside by another graphene layer on a copper foil. The copper foil was lifted gradually to ensure that the new graphene was fully covered by the film. The dissolution process of copper and the transfer operation of graphene were repeated alternatively until three layers of graphene were stacked together. Next, the three-layer graphene was transferred onto a LPFG sensor, which was fixed on a glass slide. Multiple LPFG sensors coated with the same number of graphene layers can be prepared at the same time to increase work efficiency, as shown in Fig. 1. Finally, the PMMA

layer outside the graphene layers was removed in an acetone bath to obtain the Gr-coated LPFG. The above process can be repeated to coat a three-layer graphene on the LPFG sensor each time. Transmission spectra of LPFG sensors coated with a different number of graphene layers were recorded using an optical interrogator (Micron Optics Si255). Transmission spectra of a representative LPFG sensor (no. 2 as designated later) was presented in Fig. 2.

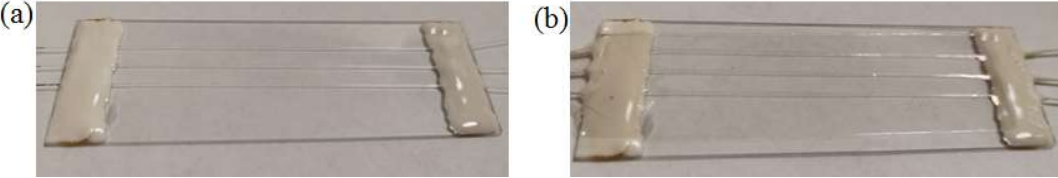


Fig. 1 Three LPFG sensors: (a) without graphene coating, (b) with graphene coating

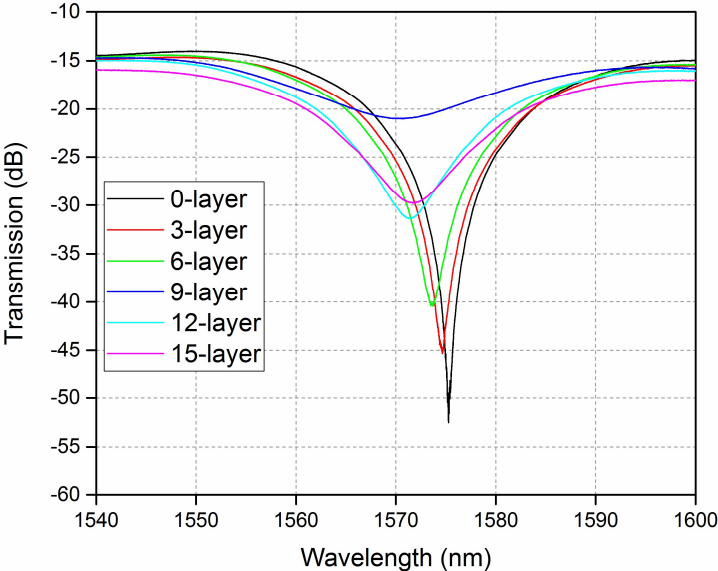


Fig. 2 Transmission spectra of a LPFG sensor coated with a varying number of graphene layers

At the beginning of sensor preparation, one LPFG sensor was broken accidentally. Thus, the test results of two LPFG sensors were reported herein. The resonant wavelengths of the two LPFG sensors coated with different numbers of graphene layers were summarized in Table 1, and the wavelength shifts were presented in Fig. 3.

Table 1 Resonant wavelengths (nm) of two LPFG sensors coated with different numbers of graphene layers

Number of graphene layers	Wavelength (nm)	
	Sensor 1	Sensor 2
0	1574.9	1575.3
3	1570.4	1574.6
6	1569.5	1573.7
9	1564.3	1570.6
12	1560.9	1571.3
15	1560.9	1571.7

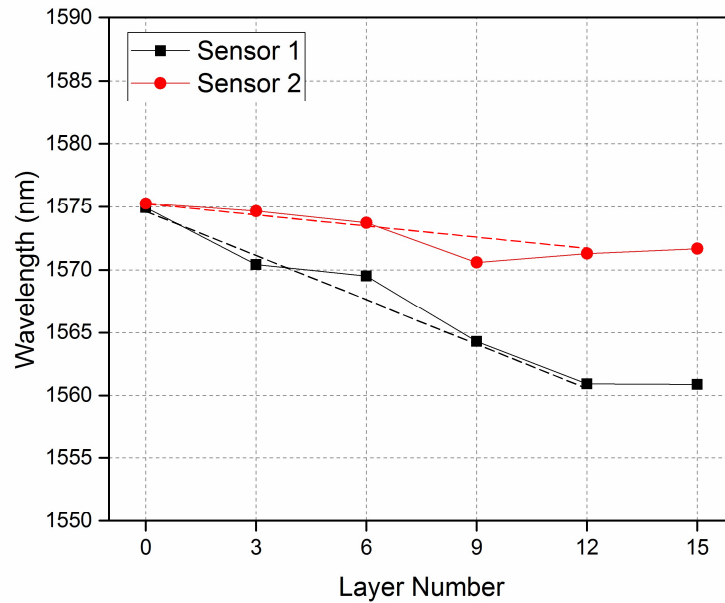


Fig. 3 Wavelength shift of two LPFG sensors with a different number of graphene layers

Fig. 3 also shows two linear trending lines (no regression analysis) between the wavelength shift of a LPFG sensor and the number of graphene layers. Overall, it can be observed from Fig. 3 that the wavelength of LPFG sensors decreased linearly with the increase in number of graphene layers. The sensitivities of the two sensors were quite different though their initial wavelengths were nearly the same. This comparison indicated a more significant bending effect in Sensor 2 for reduced sensitivity in the process of repeated graphene applications.

The wavelength shift appeared to stop when the number of graphene layers reached 12. This result indicated an evanescent field depth of approximately 4 nm. The wavelength shift of Sensor 1 corresponding to six layers of graphene seemed an outlier. The wavelength shift of Sensor 2 corresponding to nine layers of graphene seemed an outlier. As indicated by the irregular and flatten transmission spectrum shown in Fig. 2, the last added three graphene layers in Sensor 2 had a significant number of wrinkles that cause a sudden reduction of transparency and thus reduce the loss of light energy in the form of evanescence field in addition to the global bending effect. The exact reasons of these outliers in Sensors 1 and 2 are yet to be studied in the future.

Task 3 Integration and field validation of multiple FBG/EFPI and multiplexed LPFG sensors for internal and external corrosion monitoring of a pipeline with temperature compensation.

To integrate a FBG/EFPI sensor into a sensor package in field applications, two designs of the sensor have been proposed. Fig. 4(a) is a schematic illustration of the spring-based sensor enclosed by an acrylic housing. In this case, a magnet hangs on parallel springs that are fixed to the housing enclosure. The lead-in end of an optical fiber passes though the top of the enclosure and then the magnet to be in proximity to the bottom of the enclosure with a gold-coated mirror. The gap between the lead-in fiber and the mirror represents a cavity length of the Extrinsic Fabry-Perot Interferometer (EFPI). The advantage of this design is that the sensor package can be fully sealed to avoid any disturbance of potential moisture or other corrosive environments on the spring and magnet. Fig. 4(b) shows the plate-based sensor with a magnet placed on top of an elastic acrylic plate. The advantage of this design is that the distance between the magnet and the pipe wall to be monitored is so easy to control by the elastic plate that the magnet can be placed closer to the pipe in applications, and thus provide a higher accuracy in measurement results.

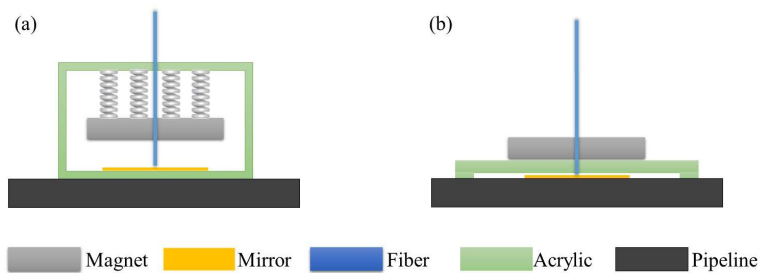


Fig. 4 Schematic illustration of two sensor package designs: (a) spring-based, and (b) plate-based

Fig. 5 shows the prototypes of two sensors for laboratory validations and calibrations. Similar to the previous tests reported in prior quarters, a steel plate with an EFPI sensor deployed on top was connected to the positive electrode in the DC circuit. Accelerated corrosion current was applied during the test and the EFPI interference pattern was recorded from an optical interrogator (Micron Optics Si 255). The cavity length between the fiber and gold coated mirror will be correlated with the mass loss of the steel plate in the following quarterly report.

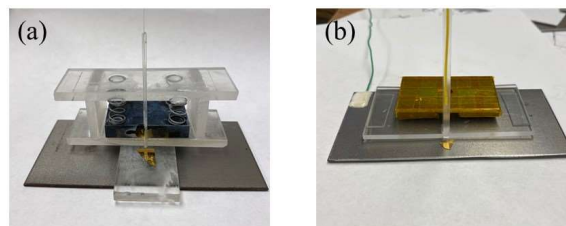


Fig. 5 Prototypes of (a) spring- and (b) plate-based sensors for laboratory tests

(c) Planned Activities for the Next Quarter - The following activities in Task 2 and Task 3 will be executed during the next reporting quarter.

Task 2 Development and validation of a graphene-based LPFG sensor with Fe-C coating for improved sensitivity in mass loss measurement in varying temperature environment

The evanescent field attenuation will continue to be characterized.

Task 3 Integration and field validation of multiple FBG/EFPI and multiplexed LPFG sensors for internal and external corrosion monitoring of a pipeline with temperature compensation.

The two robust sensor designs will be validated and calibrated for simulated field applications with temperature effects compensated by FBG sensors.

(d) Problems Encountered during this Quarter and Potential Impact on Next Quarter – This project has been impacted by the COVID-19. At Missouri S&T, laboratories were closed on March 16, 2020, and re-opened on June 1, 2020 with social distancing and hand sanitizing practices in mind. To keep six feet apart between any two students in laboratory, limited laboratory access is available to students. As such, students may have to work in shift.